**Journal of International Scientific Publications: Materials, Methods and Technologies**

Volume 8, ISSN 1314-7269 (Online), Published at: http://www.scientific-publications.net

# EVALUATION OF THE BIOACTIVITY PROPERTIES OF SILVER DOPED HYDROXYAPATITE DEPENDING ON THE PREPARATION METHOD

L.Poca, A.Dubnika, D.Loca and L.Berzina-Cimdina

Institute of General Chemical Engineering, Riga Technical University, Paula Valdena Str. 3,

Riga, Latvia, LV-1048

**Abstract**

*In the present study in vitro bioactivity properties of silver doped hydroxyapatite (HAp/Ag) ceramic scaffolds were evaluated. HAp/Ag powder samples with 0.3 - 2.0 wt % of silver were prepared by two different modified wet precipitation methods at 90 $^{o}$C temperature. The Obtained fine HAp/Ag powder was used to prepare dense and porous HAp/Ag ceramic scaffolds. The bioactivity properties of dense and porous HAp/Ag ceramics scaffolds were determined in simulated body fluid (SBF). The scanning electron microscopy (SEM) investigations showed a nucleation process of calcium containing crystals and formation of bone-like apatite layer on the surface of HAp/Ag ceramic scaffolds. SEM microphotographs showed that the formed apatite layer on the dense HAp/Ag scaffolds was thicker if compared with porous HAp/Ag ceramic scaffolds. Significant differences in the formation process of bone-like apatite layer could be attributed to the differences of scaffold porosity, surface morphology and distribution of silver particles throughout the HAp/Ag ceramic scaffolds.*

**Key words:** *hydroxyapatite, silver, in vitro, bioactivity, SBF solution*

## 1. INTRODUCTION

Calcium phosphate based biomaterials, particularly hydroxyapatite, have a wide range of applications in orthopedic and maxillofacial surgeries and dentistry (Hench 1998; Dorozhkin 2010). Synthetic hydroxyapatite is known for its excellent bioactivity, good osteoconductivity and biocompatibility; therefore it is used in medical applications for bone regeneration as an implant material (Vallet-Regi 2001; Dorozhkin 2009). Hydroxyapatite is stable in the physiological solutions and after implantation it can support bone ingrowth and osseointegration (Shi 2006; Jallot 1998).

After implantation bacterial adhesion on the implant material surface can be observed (Venegas, Palacios, Apella, Morando & Blesa 2006). The bacterial infections are considered as the main reason which can lead to the complication after implantation or implant material rejection of the human body. To minimize the infection risk the implant materials are covered with biologically compatible materials or antibacterial agents are incorporated within the chemical structure of the implant material (Ruchholtz, Tager & Nast-Kolb 2004; Campoccia, Montanaro & Arciola 2006).

Several studies describe that metal ions like $Ag^{+}$ are used for a long time in the biomedical field as antibacterial agents (Blaker, Nazhat & Boccaccini 2003; Kim, Feng, Kim, Wu, Wang, Chen & Cui 1998; Feng, Cui, Kim & Kim 1999). *In vitro* silver is toxic for bacteria, algae, and fungi. Among that silver has oligodynamic effect; silver is the least toxic to living body. The effectiveness of silver as an antibacterial agent is based on the ability of the biologically active silver ion to irreversibly damage the enzyme systems in the cell membranes of bacteria (Lansdown 2006; Maillard & Hartemann 2013; Fung & Bowen 1996). The combination of silver and hydroxyapatite properties leads to an implant material, which is capable to prevent infections.

In recent years, special attention has been paid to the porous HAp ceramic production. Porous HAp ceramics are bone substitute materials, which can imitate the natural bone mineral phase micro- and macrostructures. These ceramics are used in biomedical engineering as delivery systems for cells and drugs. After porous HAp ceramic material implantation into the living body, the bone grows into the pores and thus the mechanical strength of HAp implant increases (Sopyan, Mel, Ramesh & Khalid 2007; Sopyan & Kaur 2009). In various studies different methods, such as conversion of natural bones, ceramic foaming technique, polymeric sponge method, gel casting of foams, microwave processing can be used to produce porous HAp ceramics (Sopyan, Mel, Ramesh & Khalid 2007), but there is a lack of information about the silver doped hydroxyapatite porous ceramic scaffold preparation process. Due to that in this study we prepared porous HAp/Ag scaffolds and determined their bioactivity properties in simulated body fluids as well as prescribed the apatite layer formation process on the

surface of HAp/Ag ceramic scaffolds. The aim of this study was to obtain dense and porous HAp/Ag ceramic scaffolds and determine their *in vitro* bioactivity properties.

## 2. MATERIALS AND METHODS

### *2.1. Synthesis of silver doped hydroxyapatite*

In this study we propose two (A and B) different modified wet precipitation methods for obtaining the silver doped hydroxyapatite (HAp/Ag) (Dubnika, Loca, Reinis, Kodols & Berzina-Cimdina 2013; Dubnika, Loca, Salma, Reinis, Poca & Berzina-Cimdina 2013). All the raw materials for method (A): calcium nitrate ($Ca(NO_3)_2 \cdot 4H_2O$; purity ≥ 99%), diammonium hydrogen phosphate ($(NH_4)_2HPO_4$; purity ≥ 98%), ammonia hydroxide solution ($NH_4OH$; purity ≥ 98%) and silver nitrate ($AgNO_3$; purity ≥ 99%), were purchased from Sigma Aldrich and used without further purification. But in the case of second method (B) calcium oxide (CaO; FLUKA, purity ≥ 97%), phosphoric acid ($H_3PO_4$; Sigma Aldrich, purity ≥ 85%) and silver nitrate ($AgNO_3$; Sigma Aldrich, purity ≥ 99%) was used as precursors. Deionised water was used for both methods. In all synthesis the amount [Ca+Ag] = 0.25 mol and the atomic ratio of (Ca+Ag)/P = 1.67 was applied. The amount of silver nitrate with atomic ratios Ag/(Ag+Ca) = 0.003 and 0.020 in the method (A) was added, but in the case of method (B) the amount of $AgNO_3$ with atomic ratios Ag/(Ag+Ca) = 0.007 and 0.010 was added.

In the case of synthesis method (A) the required amount of $Ca(NO_3)_2 \cdot 4H_2O$ ($c_M$ = 0.25 mol/L) was dissolved in water, afterwards the required amount of dissolved silver nitrate solution ($c_M$ = 0.01 mol/L) was added. The obtained solution was stirred (at the rate of 220 rpm) at 90 $^oC$ for 2 h. During the synthesis process, diammonium hydrogen phsopahte was added dropwise at the rate of 4.2 mL/min. Ammonia hydroxyide solution was added at rate of 1.3 mL/min and the pH of the solution was controlled.

While, in the case of synthesis method (B), calcium hydroxide ($Ca(OH)_2$, $c_M$ = 0.25 mol/L) suspension was prepared by milling the required amount of CaO in 200 mL of deionised water in a ball mill. Silver nitrate was dissolved in water ($c_M$ = 0.01 mol/L) and added to the $Ca(OH)_2$ suspension. Then the suspension was heated up to 90 $^oC$ with continuous stirring. The obtained synthesis solution was stirred at 90 $^oC$ for 2 h. During the synthesis process, $H_3PO_4$ ($c_M$ = 2.0 mol/L) was added dropwise to the synthesis suspension and synthesis solution pH was controlled.

The obtained suspensions from both (A) and (B) methods were aged for 15 h, filtered/centrifugated and obtained precipitates were dried for 18 h and milled to obtain a fine powder. Obtained HAp/Ag powder was used to prepare dense and porous ceramic scaffolds. For the preparation of dense samples HAp/Ag powder was uniaxially pressed (F= 5 kN) in 2 mm thick (Ø = 10 mm) scaffolds. HAp/Ag powder (49 wt%), glycerol ($C_3H_5(OH)_3$); purity ≥ 99.8%, BIO-VENTA) with 50 wt%, water and ammonium bicarbonate ($NH_4HCO_3$; ES/BASF, ENOLA) with 1 wt% was used for the preparation of porous scaffolds with *in situ* foaming method (Locs, Zalite, Berzina-Cimdina & Sokolova 2013). $NH_4HCO_3$ was used as pore forming agent with particle size in the range from 100 – 300 μm. The obtained viscous mass was placed in the polyurethane cylindrical molds (with a diameter of 10 mm) and heated up to 120 $^oC$ temperature. Prepared porous and dense HAp/Ag scaffolds were sintered at 1000 $^oC$ temperature for 2 h. All synthesis was repeated at least three times.

### *2.2. Silver doped hydroxyapatite sample characterization*

Silver doped hydroxyapatite powders were analyzed by X-ray powder diffraction (XRD) using Cu Kα radiation at 40 kV and 30 mA, 2θ range of $10^o$ - $55^o$. The phase identification was made by XRD phase identification software HighScore. To evaluate the surface morphology of HAp/Ag ceramic scaffolds, scanning electron microscopy (SEM) was used. X-ray flurorescence spectrometry (XRF, BRUKER, Pioneer S4, Rh tube a voltage of 4 kW, P10 detector gas) was used to determine the silver content in the HAp/Ag powder samples. The porosity of HAp/Ag ceramic scaffolds was measured using the Archimedes method.

### *2.3. Evaluation of silver doped hydrxyapatite scaffold bioactivity*

Bioactivity of dense and porous HAp/Ag ceramic scaffold were determined in simulated body fluid (SBF) prepared regarding the Kokubo methodology (Kokubo 2008; Kokubo & Takadama 2006). Briefly, the SBF solution was prepared by dissolving appropriate quantities of the reagent-grade salt components: NaCl (Sigma Aldrich; purity ≥ 98%), $NaHCO_3$ (Sigma Aldrich; purity ≥ 95%), KCl (Sigma Aldrich; purity ≥ 98%), $K_2HPO_4 \cdot 3H_2O$ (Sigma Aldrich; purity ≥ 98%), $MgCl_2 \cdot 6H_2O$ (Sigma Aldrich; purity ≥ 99%), $Na_2SO_4$ (FLUKA; purity ≥ 99%) and $CaCl_2 \cdot 2H_2O$ (Sigma Aldrich; purity ≥ 95%) in deionized water. All salt components were used without further purification. The reagent $(CH_2OH)_3CNH_2$ (Sigma Aldrich; purity ≥

99.8%), was used to buffer the SBF solution, and the pH value was adjusted to 7.45 ± 0.01 at 36.5 ± 0.5 $^{o}$C by adding 0.1 M HCl before the addition of $CaCl_2$ (Sigma Aldrich; purity ≥ 95%), to prevent the formation of precipitates. The dense and porous HAp/Ag ceramic scaffolds were incubated in 15 mL of SBF, maintained at 37.0 ± 1.0 $^{o}$C. The HAp/Ag samples were evaluated after 7, 14, 30 and 60 days. SBF solution was continuously replaced every 3 days. All experiments were performed in triplicate, by placing three parallel independent HAp/Ag ceramic scaffolds simultaneously in the SBF.

## 3. RESULTS AND DISCUSSION

### *3.1. Characterization of silver doped hydroxyapatite*

In the present study, the silver doped hydroxyapatite crystalline phase composition changes were identified by XRD. The XRD patterns of sintered HAp/Ag powders at 1000 $^{o}$C temperature are shown in Fig. 1. The obtained powder samples (A_HAp and A1_HAp) synthesized by method (A) contain two crystalline phases – HAp and Ag; the characteristic peaks of silver were observed at 2θ 38.2$^{o}$ and 44.4$^{o}$. Obtained powder samples (B_HAp and B1_HAp) synthesized by method (B) contain three different crystalline phases - HAp, Ag and AgO; the characteristic peak of silver oxide was observed at 2θ 37.5$^{o}$. The obtained silver doped hydroxyapatite powders were used to prepare dense and porous HAp/Ag ceramics scaffold. Porosity and *in vitro* bioactivity properties of obtained HAp/Ag ceramic scaffolds were determined.

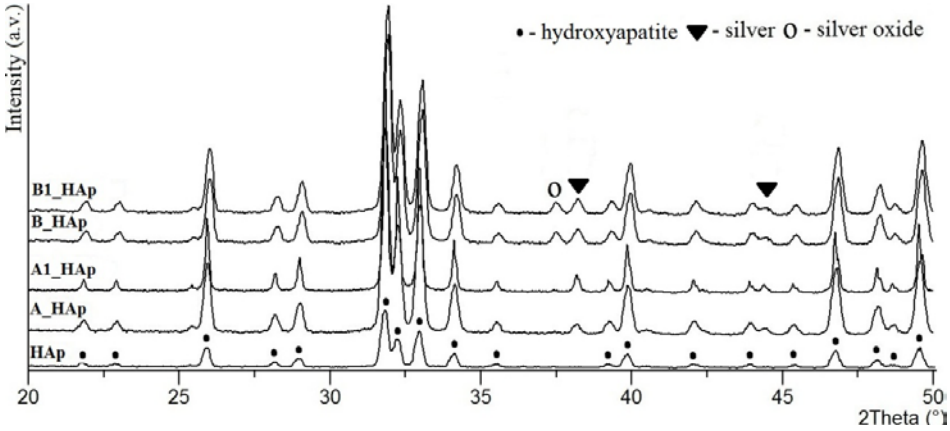


Fig. 1. XRD patterns of the HAp and HAp/Ag powder samples.

The silver content in HAp/Ag powders was evaluated with XRF. XRF results (Table 1) showed that silver content in obtained HAp/Ag powders was lower than added silver amount during the synthesis process. The silver recovery decreased from 47% to 17%. The recovery of A_HAp and A1_HAp powder samples was lower between 17 - 47 % than the recovery of B_HAp and B1_HAp powder samples. These results indicate that stable complex ion $[Ag(NH_3)_2]^+$ was built during the synthesis in case of method (A) therefore less silver ions could be incorporated within the HAp structure.

Table 1. Silver content in HAp/Ag powders

| Powder sample | Silver content [wt%] | | Recovery (%) |
|---|---|---|---|
| | Added during synthesis process | As-synthesized powder | |
| A_HAp | 0.3 | 0.14±0.01 | 47 |
| A1_HAp | 2.0 | 0.35±0.03 | 17 |
| B_HAp | 0.7 | 0.43±0.03 | 61 |
| B1_HAp | 1.0 | 0.30±0.02 | 30 |

Porosity results showed that total porosity of dense HAp/Ag ceramic scaffolds (Fig. 2.) was from 37 % to 52 %, while the open porosity was from 27 % to 38 %. The total porosity of dense HAp/Ag scaffolds was similar for both synthesis methods. The open porosity results of HAp/Ag scaffolds prepared by method (A) approved that these samples are with higher density and have less open pores comparing to the HAp/Ag scaffolds prepared by synthesis method (B).

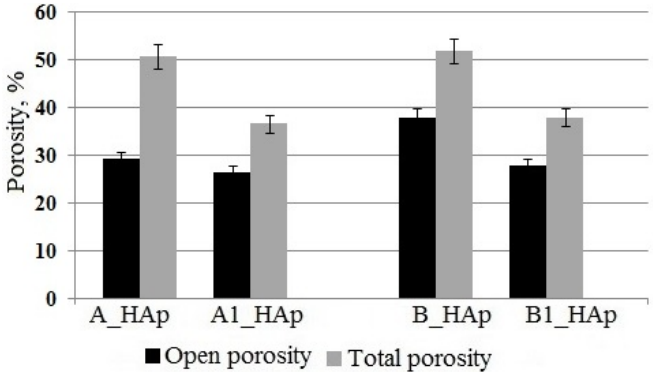


Fig. 2. The porosity (%) of dense HAp/Ag ceramic scaffolds.

The total porosity of porous HAp/Ag ceramic scaffold was ~30 % higher than for dense scaffolds (Fig. 3.). The open porosity of HAp/Ag scaffolds prepared by method (B) was 20 % higher than for HAp/Ag scaffolds prepared by method (A). Due to that B_HAp and B1_HAp samples could be more suitable as drug delivery systems (Loca, Locs, Gulbis, Salma & Berzina-Cimdina 2011).

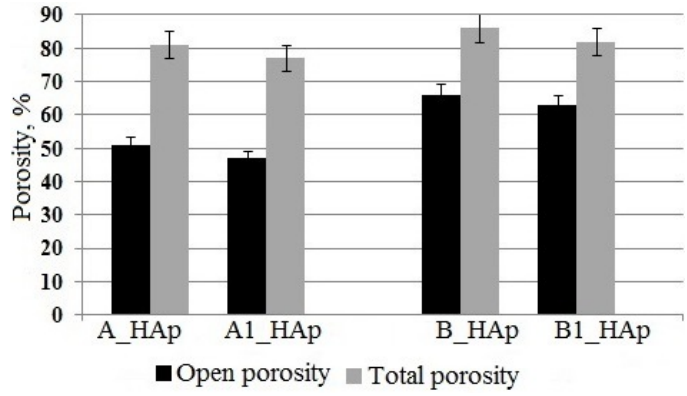


Fig. 3. The porosity (%) of porous HAp/Ag ceramic scaffolds.

The SEM microphotographs of HAp/Ag ceramic scaffold surfaces are shown in Fig. 4. It was observed that fracture morphology of dense HAp/Ag scaffolds was fine grained, grains were closely compacted to each other and only some micropores were formed. In the fracture of dense scaffolds the silver particles were observed (Fig. 4 A and B).

Surface morphology of porous HAp/Ag ceramic scaffolds after sintering at 1000 $^{o}$C temperature for 2 h is shown in Fig. 4 C and D. Macropores and micropores within the porous scaffold fractures were identified. Silver particles are displaced on the porous HAp/Ag scaffold surfaces during the sintering process. Figure 4 D shows that porous ceramic scaffold which were prepared by synthesis method (B) in cross-section had more silver particles than porous ceramic scaffold which were prepared by synthesis method (A) in Fig. 4 C. Also, the silver particles were equally distributed on surface of HAp/Ag scaffold which were prepared by synthesis method (B).

*3.2. Bioactivity properties of silver doped hydroxyapatite*

The SEM microphotographs showed a nucleation process of calcium containing crystals. The formation of bone-like apatite layer of HAp/Ag ceramic scaffold surfaces was determined. The formation process of bone-like apatite layer on all HAp/Ag ceramic scaffold surfaces in SBF media was similar to the formation process apatite layer on pure HAp (Kim, Himeno, Kokubo & Nakamura 2005). HAp/Ag ceramic scaffolds were incubated in 15 mL of SBF for various periods of time – 7, 14, 30 and 60 days. The weight changes of dense and porous HAp/Ag ceramic scaffolds during the incubation process were determined and apatite layer formation on the scaffolds was measured during the research with SEM. Obtained SEM results were compared to mass changes of all scaffolds.

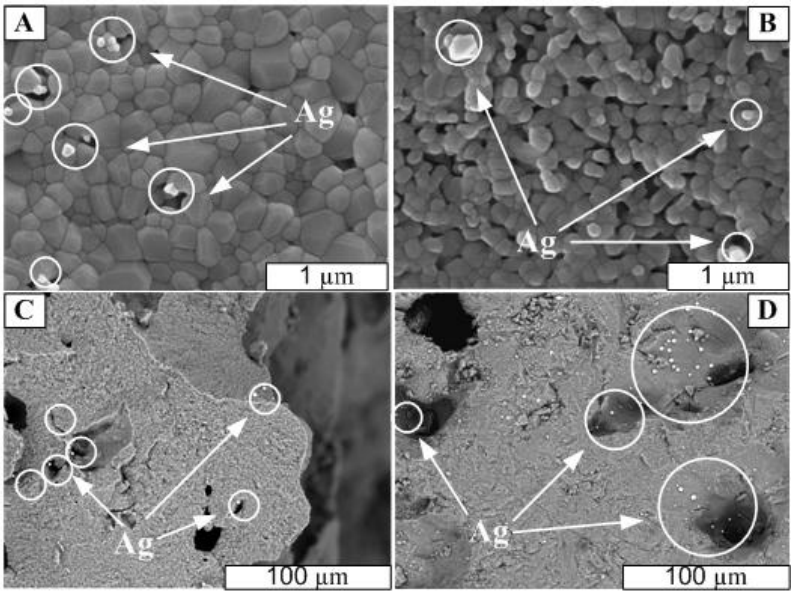


Fig. 4. Surface morphology: A and B - of dense HAp/Ag scaffolds;

C and D – of porous HAp/Ag scaffolds.

The weight changes for all HAp/Ag ceramics scaffolds were with similar trends. The average weight of dense HAp/Ag ceramic scaffolds increased by 9.5 % but for porous HAp/Ag ceramic scaffolds by 8.3 % (Table 2) after 60 days of incubation in SBF. The average weight of dense HAp/Ag ceramic scaffold which were prepared by synthesis method (A) was ~ 12% while that of dense HAp/Ag ceramic scaffold which were prepared by synthesis method (B) was only ~ 8 %. If we compare porous ceramic scaffolds, the average weight prepared by method (A) was 8%, while the scaffold prepared by method (B) was ~ 9%. The apatite layer formation on the HAp/Ag scaffold surfaces strongly depends on the ceramic scaffold preparation technology. SEM microphotographs showed that formed apatite layers on the dense HAp/Ag scaffolds were thicker if compared with porous HAp/Ag ceramic scaffolds. Significant differences in the apatite layer formation process could be attributed to the differences in the HAp/Ag ceramic scaffold porosity, surface morphology and also silver particle distribution throughout the porous and dense scaffolds.

The formation process of apatite layer affected weight changes of HAp/Ag ceramic scaffolds. The average weight of dense HAp/Ag ceramic scaffold increased by ~ 7 % after 14 days of incubation in SBF if compared with first day, but bone-like apatite layer on scaffolds increased by ~ 5.5 µm (Table 2). The average weight of porous HAp/Ag ceramic scaffold increased by ~ 5 % after 14 days of incubation in SBF. At the same time ~ 1.7 µm thick apatite layer was formed on the surface of scaffold. By comparing the HAp/Ag ceramic scaffold after 14 days of incubation in SBF, it was observed that thickness of apatite layer on dense scaffolds was about 70 % higher than the apatite layer thickness on porous scaffolds.

By comparing the dense HAp/Ag scaffold surface morphology before and after incubation in SBF for 7 days, it was observed that dense HAp/Ag scaffold surface interacts with the SBF solution and needle-like crystals were

formed on the scaffolds surface (Fig. 5). This crystals formation process corresponds to an amorphous calcium-poor apatite layer formation mechanism (Kokubo & Takadama 2006).

Table 2. Weight changes and apatite layer thickness of HAp/Ag scaffolds after incubation on SBF

| Sample | Weigh changes, % | | | | Apatite layer thickness on the scaffold surfaces, μm | | | |
|---|---|---|---|---|---|---|---|---|
| | After 7 days | After 14 days | After 30 days | After 60 days | After 7 days | After 14 days | After 30 days | After 60 days |
| Dense HAp/Ag ceramic scaffolds | | | | | | | | |
| A_HAp | 0.9 | 5.0 | 6.0 | 10.0 | - | 5.96 | 12.46 | 20.12 |
| A1_HAp | 1.0 | 5.0 | 7.0 | 13.0 | - | 6.73 | 18.02 | 32.20 |
| B_HAp | 1.0 | 9.0 | 7.0 | 8.0 | - | 4.48 | 11.05 | 18.67 |
| B1_HAp | 1.0 | 9.0 | 6.0 | 7.0 | - | 5.03 | 11.85 | 18.52 |
| Porous HAp/Ag ceramic scaffolds | | | | | | | | |
| A_HAp | 2.0 | 5.0 | 5.0 | 6.0 | - | 1.08 | 8.71 | 18.74 |
| A1_HAp | 2.0 | 5.0 | 8.0 | 9.0 | - | 2.85 | 12.76 | 28.73 |
| B_HAp | 1.0 | 4.0 | 9.0 | 10.0 | - | 1.02 | 2.16 | 8.90 |
| B1_HAP | 1.0 | 5.0 | 7.0 | 8.0 | - | 1.67 | 4.71 | 13.45 |

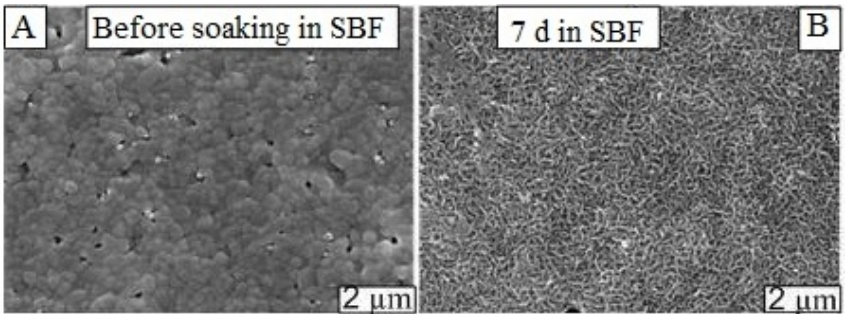


Fig. 5. Surface morphology of dense HAp/Ag scaffolds:

A - before incubation in SBF; B – after 7 days of incubation in SBF.

After 14 days of incubation in SBF dense HAp/Ag scaffolds were coated with a heterogeneous apatite layer with an average thickness of 6 μm (Table 2). By increasing the incubation time bone-like apatite layer started to compact and became homogenous. The apatite layer on the dense HAp/Ag scaffolds prepared by method (A) increased three to five times if compared with first day of incubation in SBF and the thickness of the layer increased from 20 μm to 32 μm (Fig. 6.). In the case of dense HAp/Ag ceramic scaffolds prepared by method (B), the apatite layer increased about four times if compared with first day of incubation in SBF. The thickness of apatite layer was from 4 μm after 14 days of incubation in SBF up to 18 μm after 60 days of incubation in SBF. The thickness of apatite layer on A_HAp and A1_HAp samples was about 30 % thicker than on samples B_HAp and B1_HAp. It can be explained by the different silver wt% content in the HAp/Ag samples. B_HAp and B1_HAp samples contain ~ 20 % more silver and these samples release silver ions faster compared to A_HAp and A1_HAp samples (Dubnika, Loca, Reinis, Kodols & Berzina-Cimdina 2013). The concentration of the released silver ions can inhibit the formation process of bone-like apatite layer on the B_HAp and B1_HAp scaffold surfaces.

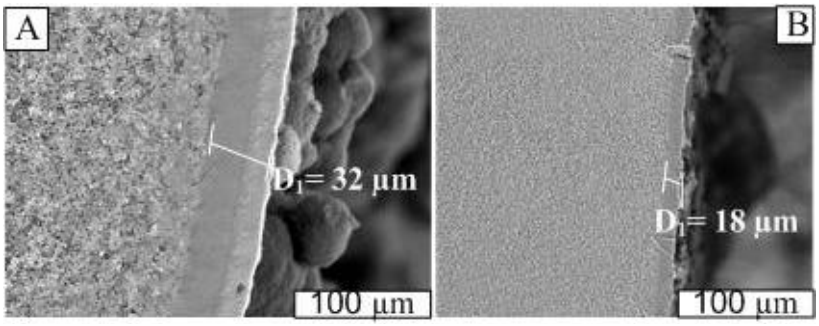


Fig. 6. Surface morphology of dense HAp/Ag scaffolds after 60 days of incubation in SBF:

A – surface of A1_HAp sample; B – surface of B1_HAp sample.

SEM investigations showed that the formation of apatite layer on the porous HAp/Ag scaffolds was slower comparing to dense HAp/Ag scaffolds. It could be attributed to the differences in scaffold surfaces, porosity and silver particle distribution throughout the scaffold volume. After 60 days of incubation in SBF, the apatite layer on A_HAp and A1_HAp porous scaffolds was coated with large apatite particle agglomerates (Fig. 7 A) and the thickness of the apatite layer reached up to 28 µm (Fig. 7 B). SEM results showed that the small apatite particles agglomerate on the surface of samples B_HAp and B1_HAp (Fig. 7 C) and the thickness of apatite layer reached up to 13 µm comparing with first day of incubation in SBF (Fig. 7 D).

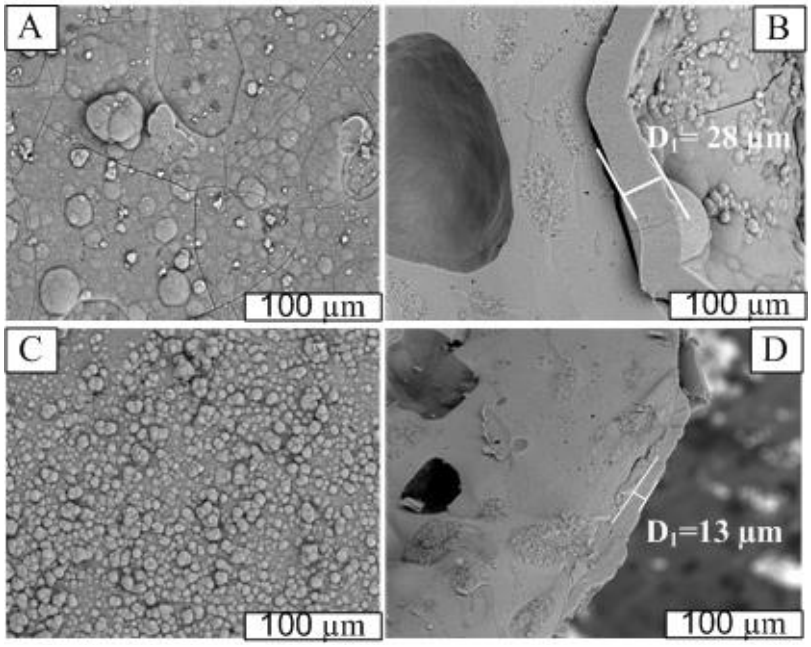


Fig. 7. Surface morphology of porous HAp/Ag scaffolds after 60 days of incubation in SBF:

A, B – surface of A1_HAp sample; C, D – surface of B1_HAp sample.

## 4. CONCLUSIONS

The formation process of apatite layer on the surface of silver doped hydroxyapatite ceramic scaffolds strongly depends on the scaffold preparation technology. A nucleation process of calcium containing crystals and the formation of bone-like layer on the HAp/Ag ceramic scaffold surfaces was determined. The average weight of dense HAp/Ag ceramic scaffold increased by 9.5 % but for porous HAp/Ag ceramic scaffold by 8.3 %. After 60 days of incubation in SBF, dense HAp/Ag scaffold surfaces were coated with bone like apatite layer (18 - 32

μm). After 1 month of incubation in SBF it was determined that the apatite layer on the surface of porous scaffolds formed much slower than on the surface of dense scaffolds, obviously due to the differences in the scaffold surface, porosity and silver particle distribution throughout the scaffold volume. Therefore, dense HAp/Ag ceramic scaffold which were prepared by synthesis method (A) showed the best ability to form apatite layer on surface. The results of thickness of bone-like apatite layer showed, that with increasing the HAp/Ag samples incubation period in SBF, the apatite layer increased from 2 μm up to 32 μm.

## ACKNOWLEDGEMENT

This work has been supported by the European Social Fund within the project «Support for the implementation of doctoral studies at Riga Technical University».

## REFERENCES

Blaker, JJ, Nazhat, SN, Boccaccini, AR 2003, 'Development and characterisation of silver-doped bioactive glass-coated sutures for tissue engineering and wound healing applications', *Biomaterials*, vol. 25, pp. 1319-1329.

Campoccia, D, Montanaro, L, Arciola, CR 2006, 'The significance of infection related to orthopedic devices and issues of antibiotic resistance', *Biomaterials*, vol. 27, pp. 2331-2339.

Dorozhkin, SV 2010, 'Bioceramics of calcium orthophosphates', *Biomaterials*, vol. 31, pp. 1465-1485.

Dorozhkin, SV 2009, 'Calcium orthophosphates in nature, biology and medicine', *Materials*, vol. 2, pp. 399-498.

Dubnika, A, Loca, D, Reinis, A, Kodols, M, Berzina-Cimdina, L 2013, 'Impact of sintering temperature on the phase composition and antibacterial properties of silver-doped hydroxyapatite', *Pure and Applied Chemistry*, vol. 85, iss.2, pp. 453-462.

Dubnika, A, Loca, D, Salma, I, Reinis, A, Poca, L, Berzina-Cimdina, L 2013, 'Evaluation of the physical and antimicrobial properties of silver doped hydroxyapatite depending on the preparation method', *Journal of Materials Science: Materials in Medicine*, doi 10.1007/s10856-013-5079-y, pp. 1-10.

Feng, QL, Cui, FZ, Kim, Kim, JW 1999, 'Ag-substituted hydroxyapatite coatings with both antimicrobial effects and biocompatibility', *Journal of Materials* Science L*etter*s, vol. 18, pp. 559-561.

Fung, MC, Bowen, DL 1996, 'Silver products for medical indications: Risk-benefit assessment', *Journal of toxicology: Clinical toxicology*, vol. 34, iss. 1, pp. 119-126.

Hench, LL 1998, 'Bioceramics', *Journal of the American Ceramic Society*, vol. 81, pp. 1705-1728.

Jallot, E 1998, 'Correlation between hydroxyapatite osseointegration and Young's Modulus', *Medical Engineering&Physics*, vol.20, iss.9, pp. 697-701.

Kim, HM, Himeno, T, Kokubo, T, Nakamura T 2005, 'Process and kinetics of bonelike apatite formation on sintered hydroxyapatite in a simulated body fluid', *Biomaterials*, vol.26, iss.21, pp. 4366-4373.

Kim, TN, Feng, QL, Kim, JO, Wu, J, Wang, H, Chen, GC, Cui, FZ 1998, 'Antimicrobial effects of metal ions ($Ag^{+}$, $Cu^{2+}$, $Zn^{2+}$) in hydroxyapatite', *Journal of Materials Science: Materials in Medicine*, vol. 9, pp. 129-134.

Kokubo, T, Takadama, H 2006, 'How useful is SBF in predicting in vivo bone bioactivity?', *Biomaterials*, vol.27, pp. 2907-2915.

Kokubo, T 2008, '*Bioceramics and their clinical applications*', Woodhead, Cambridge.

Lansdown, AB 2006, 'Silver in health care: antimicrobial effects and safety in use', *Current Problems in Dermatology*, vol.33, pp. 17-34.

Loca, D, Locs, J, Gulbis, I, Salma, I, Berzina-Cimdina L 2011, 'Lidocaine loaded Ca/Pscaffolds for bone regeneration and local drug delivery', *Advanced Materials Research*, vol.222, pp. 289-292.

Locs, J, Zalite, V, Berzina-Cimdina, L, Sokolova, M 2013, 'Ammonium hydrogen carbonate provided viscous slurry foaming –A novel technology for the preparation of porous ceramics', Journal of the *European Ceramic Society*, vol.33, iss.15-16, pp. 3437-3443.

Maillard, JV, Hartemann, P 2013, 'Silver as an antimicrobial: facts and gaps in knowledge', *Critical Reviews in Microbiology*, vol. 39, no. 4 , pp. 373-383.

Ruchholtz, S, Tager, G, Nast-Kolb, D 2004, 'The periprosthetic total hip infection', *Unfallchirurg*, vol. 107, pp. 307-317.

Shi, D 2006, '*Introduction to Biomaterials'*, World Scientific, Singapore.

Sopyan, I, Mel, M, Ramesh, S, Khalid, KA 2007, 'Porous hydroxyapatite for artificial bone applications', *Science and Technology of Advanced Materials*, vol.8, pp. 116-123.

Sopyan, I, Kaur J 2009, 'Preparation and characterization of porous hydroxyapatite through polymeric sponge method', *Ceramics International*, vol.35, iss.8, pp. 3161-3168.

Vallet-Regi, M 2001, 'Ceramics for medical applications', *Journal of the American Ceramic Society*, vol. 2, pp. 97-108.

Venegas, SC, Palacios, JM, Apella, MC, Morando, PJ, Blesa, MA 2006, 'Calcium modulates interactions between bacteria and hydroxyapatite', *Journal of Dental Research*, vol. 85, iss. 12, pp. 1124-1128.